Anal. Chem. **2001,** *73,* 103−110

Electrochemically Actuated Mercury Pump for Fluid Flow and Delivery

Jing Ni, Chuan-Jian Zhong, Shelley J. Coldiron, and Marc D. Porter*

Microanalytical Instrumentation Center, Ames Laboratory—USDOE, and Department of Chemistry, Iowa State University, Ames, Iowa 50011

This paper describes the development of a prototype pumping system with the potential for incorporation into miniaturized, fluid-based analytical instruments. The approach exploits the well-established electrocapillarity phenomena at a mercury/electrolyte interface as the mechanism for pump actuation. That is, electrochemically induced changes in the surface tension of mercury result in the pistonlike movement of a mercury column confined within a capillary. We present herein theoretical and experimental assessments of pump performance. The design and construction of the pump are detailed, and the potential attributes of this design, including the generated pumping pressure, flow rate, and power consumption, are discussed. The possible miniaturization of the pump for use as a field-deployable, fluid-delivery device is also briefly examined.

The growing need for small-sized, field/site-deployable instrumentation to function as environmental monitors in both earth- and space-based applications has stimulated a great deal of interest in the design of miniaturized analytical instrumentation.[1,2] Operationally, a reduction in size may reduce the consumption of reagents, shorten analysis times, and enhance the capability to analyze small amounts of samples.[3] Indeed, efforts to reduce significantly the size of analytical systems that are the workhorses in the modern analytical laboratory, such as flow injection analyzers (FIA),[4] capillary electrophoresis systems,[5,6] gas[7] and liquid chromatographs (LC),[8,9] and mass spectrometers,[10] have been ongoing since the 1980s.[3,11,12] These developments, many of which were triggered by breakthroughs in micromachining and microfabrication capabilities,[13,14] have led to far-reaching concepts such as the chemical analysis laboratory on a chip, electronic noses, and biochips.[15]

Of the many challenges in merging micromachining and chemical analysis technologies, the development of micropumps continues to be a key issue. Development issues include not only the construction and integration of micropumps but also the formulization of descriptions for fluid flow (i.e., microfluidics[16,17]) within exceedingly small-sized (e.g., tens of micrometers) channels. Several types of micropumps and the requisite microvalves have been devised and extensively tested along with various forms of micromixers and microdosers.[18−20] In many of the existing examples, micromachined silicon or polymer diaphragms have served as flexible physical elements that induce fluid flow via piezoelectric, pneumatic, or magnetic actuation. The limited lifetime of these diaphragms, however, remains somewhat problematic.

Recently, surface tension changes along a flow channel have been employed for fluid pumping, a concept known as Marangoni flow.[21,22] In these approaches, a surface tension gradient was generated between two electrodes positioned on the walls of the flow channel by electrolyzing surfactants,[21] immiscible electrolyte solutions,[23] or polymer gels.[22] Compared to gravitational and frictional forces, the effects of surface tension in fluidic systems become increasingly significant upon miniaturization and are

* To whom correspondence should be addressed: (telephone) (515) 294-6433; (fax) (515) 294-3254; (e-mail) mporter@porter1.ameslab.gov.

(1) Shoji, S.; Esashi, M.; van der Schoot, B. H.; de Rooij, N. *Sens. Actuators, A* **1992**, *A32*, 335.
(2) Manz, A.; Graber, N.; Widmer, H. M. *Sens. Actuators, B* **1990**, *B1*, 244.
(3) Manz, A.; Harrison, D. J.; Verpoorte, E.; Widmer, H. M. *Adv. Chromatogr.* **1993**, *33*, 1.
(4) van der Schoot, B. H.; Jeanneret, S.; van den Berg, A.; de Rooij, N. F. *Sens. Actuators, B* **1993**, *B13*, 333.
(5) Jacobson, S. C.; Hergenroder, R.; Koutny, L. B.; Ramsey, J. M. *Anal. Chem.* **1994**, *66*, 1114.
(6) Woolley, A. T.; Sensabaugh, G. F.; Mathies, R. A. *Anal. Chem.* **1997**, *69*, 2181.
(7) Terry, S. C.; Jerman, J. H.; Angell, J. B. *IEEE Trans. Electron Devices* **1979**, *26*, 1880.
(8) Manz, A.; Miyahara, Y.; Miura, J.; Watanabe, Y.; Miyagi, H.; Sato, K. *Sens. Actuators, B* **1990**, *B1*, 249.
(9) He, B.; Tait, N.; Regnier, F. *Anal. Chem.* **1998**, *70*, 3790.
(10) Barber, S. J.; Morse, A. D.; Wright, I. P.; Kent, B. J.; Waltham, N. R.; Todd, J. F. J.; Pillinger, C. T. *Adv. Mass Spectrom.* **1998**, *14*.
(11) Colyer, C. L.; Tang, T.; Chiem, N.; Harrison, D. J. *Electrophoresis* **1997**, *18*, 1733.
(12) Figeys, D.; Pino, D. *Anal. Chem.* **2000**, *72*, 330A.
(13) Mastrangelo, C. H.; Tang, W. C. In *Semiconductor Sensors*; Sze, S. M., Ed.; John Wiley and Sons: New York, 1994; p 17.
(14) Kovacs, G. T. A.; Petersen, K.; Albin, M. *Anal. Chem.* **1996**, *38*, 407A.
(15) Harrison, D. J.; van den Berg, A. *Proceedings of the Micro Total Analysis Systems '98*; Kluwer Academic: Banff, Canada, 1998.
(16) Gravesen, P.; Branebjerg, J.; Soendergaard Jensen, O. *J. Micromech. Microeng.* **1993**, *3*, 168.
(17) Liu, R. H.; Stremler, M. A.; Sharp, K. V.; Olsen, M. G.; Santiago, J. G.; Adrian, R. J.; Aref, H.; Beebe, D. J. *J. Microelectromech. Syst.* **2000**, *9*, 190.
(18) Shoji, S.; Nakagawa, S.; Esashi, M. *Sens. Actuators, A* **1990**, *A21*, 189.
(19) Lintel, H. T. G. v.; van de Pol, F. C. M.; Bouwstra, S. *Sens. Actuators* **1988**, *15*, 153.
(20) Olsson, A.; Enoksson, P.; Stemme, G.; Stemme, E. *J. Microelectromech. Syst.* **1997**, *6*, 161.
(21) Gallardo, B. S.; Gupta, V. K.; Eagerton, F. D.; Jong, L. I.; Craig, V. S.; Shah, R. R.; Abbott, N. L. *Science* **1999**, *283*, 57.
(22) Lee, H. J.; Fermin, D. J.; Corn, R. M.; Girault, H. H. *Electrochem. Comm.* **1999**, *1*, 190.
(23) Girault, H. H. J.; Schiffrin, D. J. *J. Electroanal. Chem.* **1984**, *179*, 277.

10.1021/ac0007478 CCC: $20.00
Published on Web 11/22/2000

generally dominant in the microgravity conditions encountered in outerspace. This paper describes a completely different approach for exploiting a change in surface tension for the construction of a miniaturized pump. It is based on the ability to electrochemically induce changes in the surface charge and, hence, the surface tension of a liquid metal, such as mercury, in contact with an electrolyte.[24,25]

Descriptions of the change in surface tension of mercury as a function of applied potential and electrolyte composition (i.e., electrocapillary curves) have been a long-standing research area in electroanalytical chemistry.[26] The electrocapillary curve for mercury electrodes often has a parabolic shape, where the potential corresponding to the surface tension maximum is defined as the potential of zero charge (pzc). Thus, the excess charge that accumulates at a mercury surface at applied potentials more positive or more negative than the pzc causes a decrease in surface tension, which, in turn, results in a relaxation in the curvature of a mercury drop. This shape change is the basis of the mercury beating heart laboratory demonstration[27] and has been used in optical and electrical switching applications.[28,29] The electrocapillarity of mercury has also been harnessed in a mechanical actuation process, which was first theorized by Matsumoto and Colgate in a micropump format[30] and recently used by Lee and Kim to build a micromachined mercury motor.[31] We present herein the first exploitation of this phenomenon,[24,25] which may have applicability in various microelectromechanical systems (e.g., chemical dispensers, reactors, and analyzers), to drive fluids continuously through a capillary. The potential application of this type of pump in miniaturized fluidic-based analytical instruments is briefly discussed.

EXPERIMENTAL SECTION

Chemicals. Mercury (ACS certified) was purchased from Fisher (Caution: toxic by inhalation, in contact with skin, and if swallowed) and subsequently cleaned by three passes through freshly pierced filter paper (hole of ~0.5 mm). Platinum wires (0.2-mm diameter), used to make electrical connection with the mercury pool and to serve as a counter electrode, were obtained from Aldrich and used as received. Potassium chloride (ACS certified) was also acquired from Fisher.

Mercury Pump Construction. The proof-of-concept design of the mercury pump (not to scale) is shown in Figure 1. The pump is composed of two parts: the main body and the insert. Figure 1A shows the two parts before assembly and Figure 1B provides two- and three-dimensional illustrations of the pump after assembly. The single-piece insert, shown in the upper left, consists

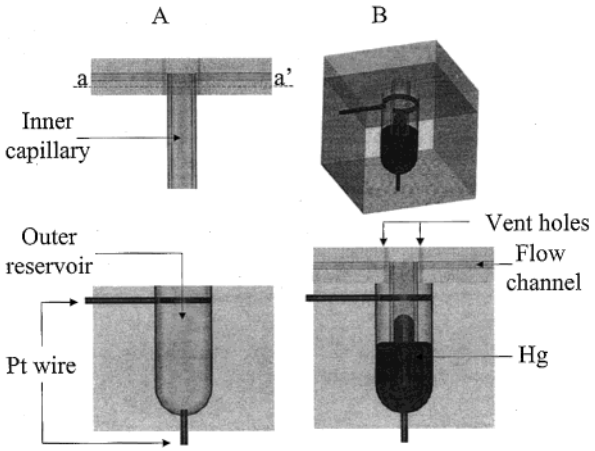

Figure 1. Proof-of-concept design for the mercury pump (not to scale). (A) Before assembly. Top: 2-D representation of the pump insert. Bottom: 2-D representation of the pump body. (B) After assembly. Top: 3-D representation of the assembled pump. Bottom: 2-D representation of the assembled pump. See Experimental Section for details.

of a 2.5 cm × 2.5 cm × 0.5 cm top platform and a cylindrically shaped, open-bottomed capillary, which defines the inner capillary. The inner capillary is 1.2 cm long. A horizontal flow channel (0.8 mm) was drilled through the top platform and opened into the inner capillary of the pump. Four small vent holes (0.2 mm) were drilled through the insert for pressure equilibration with the outer reservoir, shown in the lower left, during actuation.

The outer mercury reservoir with a depth of 1.5 cm was formed by drilling a hole into a 2.5 cm × 2.5 cm × 2.0 cm Plexiglas block. A coiled platinum wire was introduced from the side of the pump body into the outer reservoir and used as the counter electrode. Another platinum wire was inserted through the bottom of the pump body to make electrical contact with the mercury. The two wires were then connected to an external electrical source (i.e., a waveform generator or a potentiostat) to manipulate the voltage applied across the mercury/electrolyte interface. The inner and the outer radii of the inner capillary and the radius of the outer reservoir were varied as part of our assessments of factors that affect pump performance.

In assembling the pump, 50−150 μL of freshly cleaned mercury was pipetted into the outer reservoir, depending on the size of the pump. The insert and the main body were then assembled, as illustrated in Figure 1B. The assembled pump therefore consists of two concentrically aligned mercury columns, partially filling the inner capillary and the outer reservoir as a result of capillary action. An aqueous electrolyte (0.5 M KCl) was introduced into the outer reservoir through the vent holes, forming the outer mercury/electrolyte interface.

Relative Height Determinations. To determine precisely the relative height (h) of the internal and external mercury columns, the pump insert was modified by removing the flow channel section of the upper platform along the dashed line a−a′ in Figure 1. The same electrolyte was added on top of the inner mercury column to prevent the evolution of hazardous mercury vapor. A Ag/AgCl (saturated KCl) reference electrode was then inserted into the electrolyte solution in the outer reservoir, and a potentiostat (Bioanalytical Systems CV-27) was used to supply the voltage to the mercury column in a common three-electrode

(24) Porter, M. D.; Hoffman, D. K.; Zhong, C. J. Fluid Pumping System Based on Electrochemically-Induced Surface Tension Changes. Iowa State University U.S. Patent 5,472, 577, 1995.
(25) Porter, M. D.; Zhong, C.-J.; Ni, J.; Coldiron, S. J.; Tang, W. C. *SAE Tech. Pap. Ser.* **1997**, *No. 972420* (27th International Conference on Environmental Systems).
(26) Bard, A. J.; Faulkner, L. R. *Electrochemical Methods: Fundamentals and Applications*; John Wiley and Sons: New York, 1980.
(27) Lin, S.-W.; keizer, J.; Rock, P. A.; Stenschke, H. *Proc. Natl. Acad. Sci U.S.A.* **1974**, *71*, 4477.
(28) Jackel, J. L.; Hackwood, S.; Beni, G. *Appl. Phys. Lett.* **1982**, *40*, 4.
(29) Beni, G.; Tenan, M. A. *J. Appl. Phys.* **1981**, *52*, 6011.
(30) Matsumoto, H.; Colgate, J. E. *IEEE Micro Electro Mechanical Systems Workshop* **1990**, 105.
(31) Lee, J.; Kim, C.-J. *IEEE Micro Electro Mechanical Systems Workshop* **1998**, 538.

configuration. We note that both the counter and reference electrodes are located in the outer reservoir and there is no electrical connection between the inner and outer pools of electrolyte; the voltage is therefore applied only across the interface formed between the electrolyte and outer mercury column.

Two additional platinum wires were mounted on separate micromanipulators (1-μm resolution), and connected to a multimeter (Wavetek 28XT) that was set in its audible continuity test mode. To determine h, one of the wires was carefully moved toward the top of the inner mercury column and the other toward the top of the outer mercury through a vent hole. When both wires made contact with the mercury, the resulting electrical continuity triggered the audio signal from the multimeter. The difference in the readings from the two micromanipulators then represented the relative height, h. In all tests, h was determined under two conditions: when the applied voltage was near the pzc of mercury (pzc for mercury in contact with 0.1 M KCl is −0.423 V vs Ag/AgCl (saturated KCl)[32]) and when the applied voltage was 1−2 V negative of the pzc. The difference between the two values of h was defined as the change in relative height, Δh.

Flow Rate Measurements. In evaluations of flow rate, a set of ball-style check valves was attached to each end of the flow channel in the top platform with heat-shrinkable tubing. These check valves, which were manufactured by Ace Glass Inc., used 2-mm-diameter spheres made from silicon carbide. The inlet check valve was then connected to a solution reservoir with a capillary, while the outlet check valve was connected to an open-ended horizontal flow channel (0.8-mm i.d.).

Before each measurement, the fluid conduit, which includes the mercury pump, check valves, and flow channels, was primed by applying carefully a vacuum to the outlet of the flow channel with a syringe. The relative height of the solution at the inlet and the outlet was then adjusted in order to avoid gravity-induced fluid flow. Square voltage waveforms were applied to the outer mercury/electrolyte interface using a TENMA 72-3060 function generator, which induced movement of the two mercury columns. Flow velocity was determined by measuring the displacement of the fluid per unit time within the horizontal flow channel located at the outlet side of the pump. The volume flow rate (F) was then calculated by multiplying the flow velocity with the cross-sectional area of the flow channel. The volume per actuation cycle data (VPC) at low pumping frequencies (≤1 Hz) were obtained by measuring directly the displacement length of the fluid during each cycle, while those at high frequencies were calculated from the values of F. All experiments were performed at room temperature.

Power Consumption Determinations. To determine the power consumption of the mercury pumps, a voltage step was applied across the mercury/electrolyte interface potentiostatically, and the change in the double-layer charging current was immediately recorded. Theoretically, the power consumption for the pump can be determined via the applied voltage, actuation frequency, and integrated charge passed during an actuation cycle. However, only the maximum power consumption, which was estimated from the product of the change in the applied voltage and the maximum charging current, will be reported in order to obtain a general perspective on the instantaneous power consumption of the pump.

RESULTS AND DISCUSSION

Theoretical Assessment. Earlier theoretical models of the pressures generated by changes in the surface tension of mercury were used in a preliminary assessment of concept feasibility.[30,33] These models consider the situation where an open capillary is inserted into a large mercury pool and subsequently filled with mercury by capillary action. In this situation, the mercury confined within the capillary exhibits capillary depression. The fundamental relationships that correlate changes in surface tension ($\Delta\gamma$), changes in relative height of the mercury column (Δh), and changes in pressure across the mercury/electrolyte interface (ΔP) are given by the formulations of Young and Laplace in eqs 1 and 2,[33]

$$\Delta h = 2\,\frac{\Delta\gamma}{R\rho g}\cos\theta \tag{1}$$

$$\Delta P = \rho g \Delta h \tag{2}$$

where R is the inner radius of the capillary, ρ is the density of mercury, g is the gravitational acceleration, and θ is the contact angle at the mercury/capillary wall interface. These equations describe the equilibrium relationship between interfacial and gravitational forces within the capillary.

If $\Delta\gamma$-induced ΔP can be utilized to drive liquid flow, the predicted ΔP can then be used to determine the flow rate (F) based on eq 3, which relates F and ΔP in terms of the radius of

$$F = \frac{\pi r^4}{8\eta_m}\,\frac{\Delta P}{L} \tag{3}$$

the flow channel (r), the viscosity of the pumped fluid (η_m), and the length of the flow channel (L).[34]

Collectively, these equations show that the fluid flow rate can be manipulated by controlling $\Delta\gamma$. That is, the greater $\Delta\gamma$, the larger Δh and ΔP, and the higher the value of F. Moreover, eqs 1 and 2 point to an important attribute of miniaturization—by reducing the radius of the capillary (R), a higher ΔP can be achieved for the same $\Delta\gamma$.

Flow rates were calculated based on these equations for conditions typically employed in miniaturized FIA and LC applications. With FIA, flow channels usually have a r of ∼250 μm and an F of a few hundreds of microliters per minute.[35] In miniaturized, open tubular LC systems, however, the flow channels are much smaller (r of 5−10 μm) as are the flow rates (F of a few nL/min.[2,3]). Table 1 summarizes the theoretical Δh, ΔP, and F results that were calculated with channel dimensions mimicking those in FIA or LC applications. In these calculations, we assumed a θ of 0°, a L of 10 cm, a η_m of 1×10^{-3} N·s·m^{-2} (i.e., the viscosity of water), and set r equal to R. The calculation also used a $\Delta\gamma$ of 100

(32) Wrona, P. K.; Galus, Z. In *Encyclopedia of Electrochemistry of the Elements*; Bard, A. J., Ed.; Marcel Dekker: New York, 1982; Vol. 9.

(33) Adamson, A. W. *Physical Chemistry of Surfaces*; John Wiley and Sons: New York, 1990.

(34) Giancoli, D. C. In *Physics: Principles with Applications*; Prentice-Hall: Englewood Cliffs, NJ, 1980; p 147.

(35) Ruzicka, J. *Flow Injection Analysis*; John Wiley and Sons: New York, 1988.

Table 1. Theoretical Assessment for Performance Figures of Merit Using a Mercury Pump Based on Electrochemically Induced Changes in Surface Tension[a,b]

R, r (μm)	Δh (cm)	ΔP (psi)	F (μL/min)
500	0.3	0.06	5890
250	0.6	0.12	736
50	3	0.58	5.89
25	6	1.16	0.736
5	30	5.80	5.89×10^{-3}

[a] This assessment is based on the situation where an open capillary is inserted into a large mercury pool. [b] Values of Δh, ΔP, and F are based on a $\Delta\gamma$ of 100 dyn/cm, θ of 0°, η_m of 1×10^{-3} N-s-m^{-2}, ρ of 13.6×10^3 kg/m^3, g of 9.8 N/kg, and L of 10 cm.

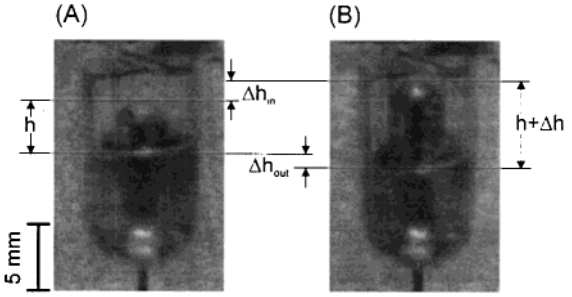

Figure 2. Photographs of the electrochemically induced actuation of the two mercury columns in pump 2. Captured at two different applied potentials: (A) −1.8 V vs Ag/AgCl (saturated KCl), which is ∼1.4 V negative of the pzc, (B) −0.4 V vs Ag/AgCl (saturated KCl), which is near the pzc. The supporting electrolyte was 0.5 M KCl.

dyn/cm, a change easily accessible when mercury is in contact with aqueous electrolytes (e.g., 0.1 M KCl).[32]

The results in Table 1 demonstrate that the pump can theoretically function in both types of analytical formats. For example, with both r and R equal to 250 μm, a $\Delta\gamma$ of 100 dyn/cm results in a ΔP of 0.12 psi and F of almost 740 μL/min. In contrast, setting r and R equal to 5 μm results in a ΔP of 5.80 psi and F of almost 6 nL/min. These results, which demonstrate the intricate interplay between R, ΔP, and F, support the possible applicability of our pump concept in both miniaturized FIA and LC.

Experimental Performance Evaluations. Building on the results of the feasibility assessments, the pump shown in Figure 1 was constructed and tested. This design, which differs from that used in the theoretical assessment in the last section, confines the outer mercury pool within a reservoir, whose internal radius is slightly larger than the external radius of the inner capillary. Under open circuit conditions, h reflects the balance of forces from gravity and surface tension. As a consequence of changing the relative radii of the capillaries, the resulting pressure differential can force the inner mercury column to rise to a height greater than that of the outer mercury column. The actuation of the pump relies on how the surface tension of the outer mercury column is altered through changes in the voltage applied across the outer mercury/electrolyte interface. This change in surface tension causes both mercury columns to reposition until a new balance between gravity and surface tension is established. It is the height change of the inner mercury column that can be exploited to displace the fluid within the flow channel. The following examines how the displacement of the inner mercury column as a function of applied voltage can be harnessed to pump fluids. The power consumption of the pump is then estimated, and a brief discussion of the possible use of this pump in a microfluidics system is presented.

(i) ΔP and Δh. The first set of experiments examined the influence of applied voltage on ΔP and Δh. As mentioned earlier, the voltage is applied across the outer mercury/electrolyte interface, indicating that only the outer mercury surface tension is affected by a change in the applied voltage (ΔE). This change in surface tension ($\Delta\gamma$) leads to a pressure change in the outer reservoir (ΔP), which causes the two mercury columns to move until a new pressure balance is established by the change in relative height (Δh) of the inner and outer mercury columns. Therefore, Δh is a reflection of the electrochemically induced ΔP, and it is a consequence of the displacement of both the inner (Δh_{in}) and the outer (Δh_{out}) mercury columns.

The actuation process of the mercury pump is demonstrated by the two photographs in Figure 2. These photographs were taken when either −1.8 (Figure 2A) or −0.4 V (Figure 2B) was applied to the mercury pool with respect to a Ag/AgCl (saturated KCl) reference electrode; 0.5 M KCl was used as the supporting electrolyte. Considering the pzc for mercury is around −0.4 V vs Ag/AgCl (saturated KCl),[32] Figure 2A, therefore, shows the relative height between the inner and outer mercury columns at an applied voltage that is ∼1.4 V negative of the pzc. Figure 2B, on the other hand, represents the relative heights at an applied voltage that is close to the pzc. Based on the electrocapillary curve for mercury in 0.1 M NaCl,[36] this difference in applied voltage induces a $\Delta\gamma$ of ∼200 dyn/cm, which, as shown in Figure 2, results in a Δh of ∼2.6 mm. This height change corresponds to an elevation of the inner mercury column (Δh_{in}) by nearly 1.5 mm and to a lowering of the outer mercury column (Δh_{out}) by ∼1.1 mm. It is Δh_{in} that directly causes the pistonlike displacement of the liquid in contact with the inner mercury column and forms the basis of fluid pumping.

The general shape of an electrocapillary curve, when combined with the predictions of eq 1, suggests that Δh can be manipulated by controlling ΔE. Our tests have shown that changing the negative limit of the applied voltage to −1.0 V, instead of the −1.8 V used for the experiment in Figure 2A, reduces Δh by more than 50% to ∼1.1 mm. We note, however, that the maximum Δh is limited by the most negative voltage that can be applied across the mercury/electrolyte interface before hydrogen evolution, which occurs near −2.0 V vs Ag/AgCl (saturated KCl) according to a voltammetric current−potential curve. We also found, as expected, that the identity and concentration of the supporting electrolyte influenced the displacement of the two columns, but the displacements were not significantly different when using simple electrolytes (e.g., sodium vs potassium, chlorides vs nitrates) over concentration ranges between 0.1 and 1 M. Therefore, 0.5 KCl was used as the supporting electrolyte for the remainder of these experiments for comparison purposes.

Besides electrochemically controlling $\Delta\gamma$, eqs 1 and 2 also suggest that the radii of the capillaries (R) should affect Δh and therefore ΔP. To assess this effect, pumps were constructed having different values of R. The experimental Δh of each pump

(36) Grahame, D. C. *Chem. Rev.* **1947**, *41*, 441.

Table 2. Theoretical (theo) and Experimental (exp) Assessment of the Pump Performance as a Result of Variation of Inner Capillary and Outer Reservoir Dimensions, in Terms of Δh, ΔP, and Δh_{in}

pump no.	R_1 (mm)	R_2 (mm)	R_3 (mm)	R_1-R_2 (mm)	Δh (mm) theo[a]	Δh (mm) exp[b]	exp Δh_{in} (mm)	exp ΔP (psi)
1	4.00	2.48	2.02	1.52	1.39	1.05	0.74	0.02
2	4.00	3.23	1.98	0.77	2.76	2.56	1.47	0.05
3	4.00	3.50	2.02	0.50	4.24	4.18	2.00	0.08
4	1.69	1.44	0.51	0.25	8.49	8.87	6.66	0.17

[a] Values of the theoretical Δh are based on a $\Delta\gamma$ of 200 dyn/cm, θ of 135°, ρ of 13.6 × 10^3 kg/m^3, and g of 9.8 N/kg. [b] The Δh data obtained from repetitive measurements usually fell within ±0.1 mm of the presented values. Because of the critical nature of the alignment of the two columns, the variability between setups for the smallest of the pumps (i.e., pump 4) can be as large as 15% if not aligned carefully.

was then determined from the difference between h measured at −0.4 and −1.8 V vs Ag/AgCl (saturated KCl), respectively.

To calculate theoretical values for Δh, eq 1 serves as a starting point to derive the correlation between Δh and the size of the two confined mercury columns in our concentrically aligned geometry. Recognizing that the voltage is applied to the outer mercury/electrolyte interface, only the surface tension of the outer mercury column changes when the applied voltage is altered. Equation 4, which reflects a balance of the effect of gravity at the inner mercury column with the surface tension-induced change in pressure at the contact surface of the outer mercury column, can therefore be written,

$$\Delta h = \frac{2\Delta\gamma \cos\theta}{\rho g}\left(\frac{1}{R_1 - R_2}\right) \quad (4)$$

where R_1 is the radius of the outer reservoir and R_2 is the external radius of the inner capillary.

The change in relative height (Δh) is related to the pressure that can be generated by the pump. The displacement of the inner mercury column (Δh_{in}), on the other hand, defines the displacement that can be utilized to induce fluid flow. The relationship among Δh_{in}, Δh, and the dimensions of the pump is presented in eq 5, where R_3 is the internal radius of the inner capillary. The

$$\Delta h_{in} = \frac{R_1^2 - R_2^2}{R_1^2 - R_2^2 + R_3^2}\Delta h \quad (5)$$

development of eqs 4 and 5 are detailed in the Appendix.

Four different-sized pumps were constructed; their sizes and performance figures of merit are given in Table 2. The experimental Δh data were then used to determine ΔP and Δh_{in} based on eqs 2 and 5. The theoretical calculations used a $\Delta\gamma$ of 200 dyn/cm, which is representative for the voltage biases used in these experiments, and a θ of 135°, which was determined from the photographs in Figure 2.

In general, the experimental results are in good agreement with the theoretical expectations. For example, Δh increased with the decrease of $R_1 - R_2$, as expected from eq 4. We attribute the small quantitative differences between experimental and theoretical results to several factors, including the approximate values of the contact angle and the surface tension used in the theoretical calculations, the disregard of the curvature of the mercury meniscus in the height measurements, and small misalignments of the inner capillary when placed in the outer reservoir.

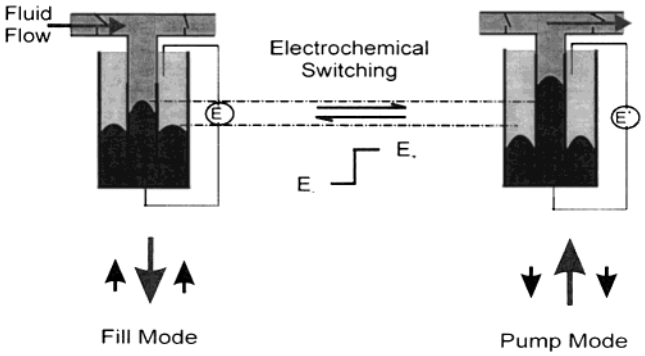

Figure 3. Schematic representation of the fill and pump modes of the mercury-based pump as a result of application of a voltage step across the mercury/electrolyte interface. The arrows below the pump conceptualize the relative displacement of the mercury in the inner and outer capillaries. By applying a voltage waveform, the movement of the mercury column within the inner capillary mimics the actuation process of a piston pump. Two check valves are incorporated in the representation to realize unidirectional fluid flow.

Most importantly, Table 2 shows that two key aspects of pump performance, ΔP and Δh_{in}, are affected by the physical size of the two containment columns, reflecting the contribution of capillarity. That is, both ΔP and Δh_{in} increase with a decrease in $R_1 - R_2$, suggesting an improved pump performance with the reduction of the separation distance between the capillaries. These results point to an important benefit of miniaturization—a decrease in size potentially enhances the ability of the pump to move fluids in microchannels.

(ii) *F*. Flow rate (F) is another important delimiter in defining pump performance. This set of experiments was aimed at delineating the flow rates accessible with our mercury-based pumps. Figure 3 conceptualizes the pistonlike actuation process for inducing fluid flow. That is, at applied voltages removed from the pzc, which is termed the "fill mode", the inner mercury column is distended and the inner capillary fills with the pumped fluid. The "pump mode", in contrast, results when the inner mercury column extends in response to an applied voltage closer to the pzc, driving fluid out of the inner capillary. Thus, the application of a waveform that oscillates between the two extremes in applied voltage induces a pistonlike reciprocation of the inner mercury column. This reciprocation can then be used for fluid delivery after incorporating check valves to realize unidirectional flow.

In the flow rate characterization, square waveforms were applied across the outer mercury/electrolyte interface in a two-electrode configuration, i.e., the mercury electrode and the platinum coil electrode inserted in the electrolyte contacting the outer mercury column. Thus, a change in the magnitude and/or frequency of the applied voltage causes a difference in the magnitude of mercury displacement and, therefore, a difference in F. Figure 4 shows the dependence of flow rate on the difference in the two limits in the applied waveform for pump 2. The amplitude of the waveform, $E_+ - E_-$ or ΔE, was manipulated by changing the negative limit (E_-) of the 1-Hz waveform after each

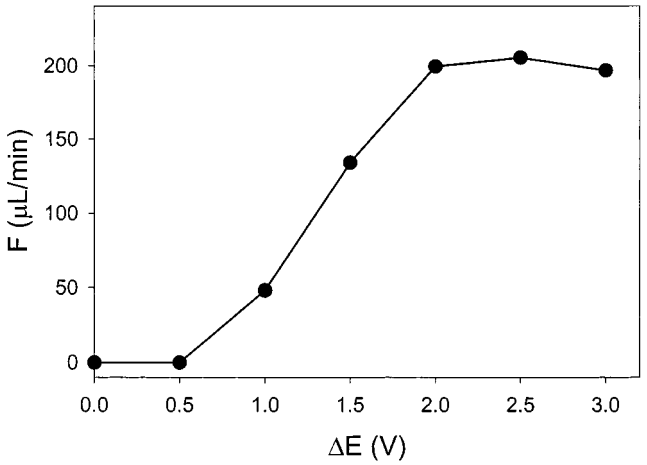

Figure 4. Dependence of flow rate on the amplitude of the applied voltage waveform for pump 2. The positive limit (E_+) of the waveform was maintained at −1.0 V, while the negative limit (E_-) was changed in each measurement. The amplitude of the square waveform (ΔE) is defined by the difference between the two voltage limits (i.e., $\Delta E = E_+ - E_-$). The frequency of the square waveform was 1 Hz, and the supporting electrolyte was 0.5 M KCl.

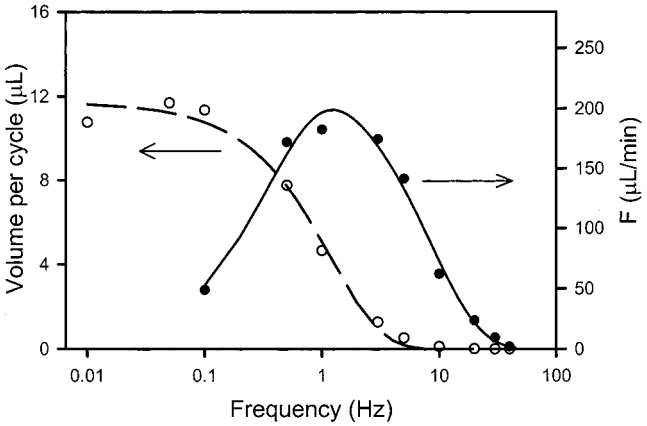

Figure 5. Dependence of volume flow rate (F, —) and volume per actuation cycle (VCP, – –) on the frequency of the applied voltage waveform measured using pump 2. The positive and negative limits of the waveform were held at −1.0 and −3.0 V, respectively. The supporting electrolyte was 0.5 M KCl.

measurement, while maintaining the same positive limit ($E_+ = -1.0$ V). The value of E_+ was chosen to be close to the pzc, while the values of E_- were moved increasingly negative of the pzc. We note that these values of E_+ and E_- are different from the values referenced against Ag/AgCl, saturated KCl in our relative height measurements, due to the different electrode configurations in the two setups.

As evident in Figure 4, applying a square waveform with lower negative limits results in a higher F. For instance, when E_- is −3.0 V (i.e., $\Delta E = +2.0$ V), F is ∼3 times larger than that observed when E_- is −2.0 V (i.e., $\Delta E = +1.0$ V). At present, the observed flow rate varies by 15% between replicate measurements using the same experimental setup. We note that a E_- lower than −3.5 V results in strong hydrogen evolution, which degrades the reliability of the flow rate determination.

Flow rates can also be manipulated by changing the frequency of the voltage waveform. A set of results from such experiments using pump 2 is shown in Figure 5 with the flow characteristics presented as both the volume per actuation cycle and the volume flow rate (F). A square waveform with E_+ at −1.0 V and E_- at −3.0 V was used to induce mercury actuation; these voltages correspond approximately to 0.0 and −1.8 V vs Ag/AgCl (saturated KCl), respectively. As is evident, F initially increases as the frequency of the waveform increases, reaches a maximum (∼175 μL/min) at ∼1 Hz, and then decreases to nearly 10% of its maximum value at 20 Hz. There is no measurable flow above 20 Hz. The value of VPC, on the other hand, exhibits a maximum (∼12 μL) at lower frequencies and starts to decrease above 0.1 Hz.

We attribute the decay of VPC and F at higher frequencies to the time constant of the pump. When modeling the mercury pump as a simple RC circuit, a nonlinear least-squares fit of the VPC dependence yields an overall time constant of ∼2 s. Two factors, the electrochemical time constant of the pump (i.e., the combined effect of electrolyte resistance and interfacial capacitance) and the inertial time constants of the mercury column and the check valves, were considered as the main contributors to the overall time constant. A voltage step experiment showed that the electrochemical time constant of a mercury electrode of similar size was less than 0.2 s, leaving the inertial drag of mercury column and/or check valves as the most likely contributors to the above observations. Since the overall weight as well as the density of mercury ($\rho = 13.6$ g/cm^3) is much higher than those of the check valves ($\rho = 2.7$ g/cm^3), we believe the decrease in performance at higher frequencies arises mainly from the inertia in inducing physical movement of mercury. In support of this conclusion, a plot of F versus the frequency of the voltage waveform for experiments using pump 4, which has smaller sized mercury columns, has a maximum for F at 5 Hz, and an actuation frequency yielding detectable fluid flow at ∼50 Hz. Moreover, we found from the VPC results that the overall time constant of this smaller pump has been reduced to 0.4 s. Since the setup for pump 4 used the same set of check valves as for pump 2, these findings demonstrate that the inertial drag of mercury is a key factor in controlling the time response. Again, a reduction in size may improve the pump performance.

(iii) Power Consumption. An experiment was also performed to develop a perspective on the power consumption of the pump. The initial peak current density after stepping the applied voltage from −0.4 to −1.8 V vs Ag/AgCl (saturated KCl) was almost 5 mA/cm^2. Therefore, the highest current flow for the pumps described in Table 2 was a few milliamperes, a level that reflects the current required to charge the electrical double layer formed by the contact between the mercury meniscus and the supporting electrolyte as the applied potential is changed. This current level, coupled with the magnitude of the change in applied voltage (1.4 V), translates to a peak power consumption of a few milliwatts. These levels of voltage and power are in contrast to electrostatic pump actuation, which consumes little power but typically requires high voltage,[5] and to electromagnetic[7] or thermal actuation,[37] which uses low voltage but operates at high power. Intriguingly, the low voltage and power consumption of our pump suggest that the small-sized power cells used in devices such as wrist watches and cameras could be adopted to operate this type of pump. The

(37) Zdeblick, M. J.; Anderson, R.; Jankowski, J.; Kline-Schoder, B.; Christel, L.; Miles, R.; Weber, W. *Solid-State Sensor and Actuator Workshop* **1994**, 251.

existence of readily available, small-sized power supplies will clearly facilitate the ongoing efforts to reduce the size of the pump to a chip-scale format.

CONCLUSIONS

In this report, we have described the capabilities of an electrochemically driven mercury pump for fluid flow and delivery. Changes in relative mercury height for pumps having several different design parameters were studied, and the experimental results showed good agreement with theoretical predictions. Flow rates up to a few hundred microliters per minute and fluid dispensing volumes as high as several tens of microliters per actuation cycle were achieved in a capillary column using mercury pumps assisted by ball-style check valves for controlling the fluid flow direction. Both the change in relative mercury height and flow rate increased proportionally to the amplitude of the voltage waveform. The low voltage requirement and power consumption of this pump may also facilitate the eventual miniaturization of the fluidic system.

Encouraged by these preliminary results, experiments to enhance performance through further optimization of the different functional elements of the pump and flow system to meet the needs of chemical analysis systems are underway. Furthermore, we believe that the potential environmental hazard of mercury can be minimized by the further reduction of the pump size and therefore the amount of mercury required for effective actuation.

ACKNOWLEDGMENT

J. N. gratefully acknowledges the support of the ACS Analytical Division Fellowship that is sponsored by the Eastman Chemical Co. We express our appreciation to Brent Dawson, Mike Granger, Jeremy Kenseth, and Robert Lipert for their assistance in manuscript preparation. This work was supported by NASA (Grant NAGW4951) and the Microanalytical Instrumentation Center of Iowa State University.

APPENDIX

This section presents the mathematical derivation for the dependence of the change in relative height, Δh (i.e., eq 4), and the inner mercury column displacement, Δh_{in} (i.e., eq 5) on the radii of the concentrically aligned inner capillary and outer reservoir. The fundamental principle underlying the Young and Laplace equations serves as the starting point of the derivation. Specifically, they suggest how surface tension and gravity affect the pressure balance inside the two mercury columns. The relative height of the two mercury columns at equilibrium therefore reflects the balance of the pressure at the inner capillary (P_{in}) and the outer reservoir (P_{out}):

$$P_{out} = P_{in} \tag{A}$$

Both pressures can be calculated using the forces that act on the mercury columns divided by their meniscus areas (A). The force at the outside column (f_{out}) can be written as the sum of the surface tensions (γ_{out}) at the inner wall of the outer reservoir and the outer wall of the inner capillary:

$$f_{out} = 2\pi(R_1 + R_2)\gamma_{out} \cos\theta \tag{B}$$

This force acts on the meniscus of the outer mercury column, the area of which can be approximated as

$$A_{out} = \pi({R_1}^2 - {R_2}^2) \tag{C}$$

The expression for P_{out} is then

$$P_{out} = \frac{2\gamma_{out}\cos\theta}{R_1 - R_2} \tag{D}$$

The total force acting within the inner column (f_{in}) at the outer meniscus height can be given as

$$f_{in} = 2\pi R_3\gamma_{in}\cos\theta + \pi {R_3}^2 h\rho g \tag{E}$$

where the first term in the equation defines the force related to the surface tension of the inner mercury column (γ_{in}) and the second term in the equation reflects the force due to the relative height (h) of the two columns. This force is applied across the surface area of the inner column (A_{in}):

$$A_{in} = \pi {R_3}^2 \tag{F}$$

The expression of P_{in} is then written as

$$P_{in} = \frac{2\gamma_{in}\cos\theta}{R_3} + \rho g h \tag{G}$$

The value of h can then be developed by equating eqs D and G and rearranging to yield

$$h = \frac{2\cos\theta}{\rho g}\left(\frac{\gamma_{out}}{R_1 - R_2} - \frac{\gamma_{in}}{R_3}\right) \tag{H}$$

Since the voltage is applied only across the outer mercury/electrolyte interface, γ_{out} changes by a value of $\Delta\gamma$. This change results in a new height difference ($h + \Delta h$) between the inner and outer mercury columns, with Δh defined as the change in relative height.

A similar set of equations (I−L) can also be written based on the pressure balance under the new equilibrium established by $\Delta\gamma$, with parameters of importance given as "primed" terms.

$$P'_{out} = P'_{in} \tag{I}$$

$$P'_{out} = \frac{2(\gamma_{out} + \Delta\gamma)\cos\theta}{R_1 - R_2} \tag{J}$$

$$P'_{in} = \frac{2\gamma_{in}\cos\theta}{R_3} + \rho g(h + \Delta h) \tag{K}$$

$$h + \Delta h = \frac{2 \cos \theta}{\rho g}\left(\frac{\gamma_{out} + \Delta\gamma}{R_1 - R_2} - \frac{\gamma_{in}}{R_3}\right) \quad \text{(L)}$$

Combining eqs H and L, and solving for Δh, gives eq 4.

The volume of fluid displaced by the pump in a single actuation step is directly related to the displacement of the inner mercury column, Δh_{in}, which can be derived from Δh through the physical dimensions of the pump. Since the total volume of the mercury inside of the pump is fixed, an increase in the volume of mercury in the inner capillary (ΔV_{in}) must equal the decrease in the volume of mercury in the outer reservoir (ΔV_{out}).

$$\Delta V_{out} = \Delta V_{in} \quad \text{(M)}$$

Each of these volume changes can be expressed as the product of the height displacement of the mercury column, and the surface area of the corresponding meniscus:

$$\Delta V_{out} = \pi(R_1^2 - R_2^2)\Delta h_{out} \quad \text{(N)}$$

$$\Delta V_{in} = \pi R_3^2 \Delta h_{in} \quad \text{(O)}$$

The above two equations can then be combined through eq M and rearranged to show the relationship between Δh_{in} and Δh_{out}:

$$\Delta h_{in} = \frac{R_1^2 - R_2^2}{R_3^2}\Delta h_{out} \quad \text{(P)}$$

Recognizing next that Δh is the direct result of Δh_{in} and Δh_{out}, we can write

$$\Delta h = \Delta h_{in} + \Delta h_{out} \quad \text{(Q)}$$

Finally, combining eqs P and Q, and solving for Δh_{in} in terms of Δh gives eq 5.

Received for review June 30, 2000. Accepted October 16, 2000.

AC0007478